

Dielectric behavior of $\text{La}_{1-x}\text{Ca}_x\text{MnO}_3$ ($0.4 \leq x \leq 0.5$)

P.M. BOTTA, J. MIRA, A. FONDADO AND J. RIVAS

Departamento de Física Aplicada, Universidade de Santiago de Compostela Campus Universitario Sur, E-15782, Santiago de Compostela, España.

In this work the dielectric behavior of semiconducting La-manganites in an intermediate Ca-doping regime is studied. Ceramic samples were prepared by conventional solid-state reaction, using elemental oxides as starting reactants. A chemical, structural and microstructural characterization of the prepared manganites was performed by iodometric titrations, X-ray diffraction and scanning electron microscopy, respectively. The magnetic susceptibility and electrical resistivity as a function of temperature were also measured. The complex dielectric permittivity of the samples was determined as a function of frequency and temperature. Very high values of dielectric constant in a wide frequency and temperature range were observed for all the synthesized samples. Moreover, an increase of the dielectric constant at temperatures close to charge-order or metal-insulator transition is reported.

Keywords: dielectric constant, manganites, charge-order, perovskites.

Comportamiento dieléctrico de $\text{La}_{1-x}\text{Ca}_x\text{MnO}_3$ ($0.4 \leq x \leq 0.5$)

En este trabajo se estudia el comportamiento dieléctrico de manganitas de La dopadas con Ca en un rango de composición cercano a 0.5. Se prepararon muestras cerámicas por el método de reacción en estado sólido, utilizando los óxidos elementales como reactivos. Los materiales obtenidos fueron caracterizados química, estructural y microestructuralmente mediante titulaciones iodométricas, difracción de rayos X y microscopía electrónica de barrido, respectivamente. Se hicieron medidas de susceptibilidad magnética y resistividad eléctrica en función de la temperatura. Además se determinó la permitividad dieléctrica compleja de las muestras sintetizadas en función de la frecuencia y la temperatura. Se observaron valores muy elevados de la constante dieléctrica en un amplio rango de frecuencias y temperaturas para todos los materiales obtenidos. También se encontró un aumento de la constante dieléctrica a temperaturas cercanas a las de las transiciones de orden de carga o metal-aislante sufridas por estos materiales.

Palabras clave: constante dieléctrica, manganitas, orden de carga, perovskitas.

1. INTRODUCTION

The development of high dielectric permittivity materials is nowadays one of the most important challenges of new technologies. This is mainly owing to the role that they play in the design of high capacitance devices, which have a double interest: on one hand, as energy storage devices and on the other hand, as capacitive elements in miniaturized circuits (1). At present, in the industrial field, the standard solution to obtain high dielectric constants has been searched in classical ferroelectric materials (2), in which exist spontaneous electric polarization due to charge separation. However, these materials exhibit a steep variation of dielectric permittivity with small temperature changes, which constitutes a severe limitation for some applications.

Recent reports of giant dielectric permittivity have directed considerable attention to several new non-ferroelectric mixed oxides and composites, such as $\text{CaCu}_3\text{Ti}_4\text{O}_{12}$ (3), percolative $\text{BaTiO}_3\text{-Ni}$ (4) and (Li,Ti)-doped NiO (5). The enormous dielectric constant of these materials seems to be a consequence of an internal barrier-layer capacitor structure (IBLC) (6), composed of insulating layers between semiconducting grains. Other reports explain the apparent colossal dielectric permittivity of these compounds by Maxwell-Wagner-type contributions of depletion layers at the interfaces between

material and contacts and/or grain boundaries (7). Studies on systems with charge condensation, such as $\text{Pr}_{2/3}\text{Ca}_{1/3}\text{MnO}_3$ (8) and $\text{La}_{3/2}\text{Sr}_{1/2}\text{NiO}_4$ (9) suggest the existence of a correlation between the dielectric properties and the electronic state in this kind of compounds.

The system $\text{La}_{1-x}\text{Ca}_x\text{MnO}_3$ has a rich magnetic phase diagram (10) where paramagnetism (PM), ferromagnetism (FM), antiferromagnetism (AFM), and charge ordering (CO) are determined by the temperature and the doping level x . Its ground state is ferromagnetic metallic for $0.15 < x < 0.5$. The phase boundary point $x = 0.5$ is a focus of great interest. Upon lowering temperature this compound first undergoes a PM to FM transition at $T \cong 225$ K, and then to a COAFM phase at temperatures between 160 and 180 K, depending on the synthesis conditions (11,12). Compounds with $0.15 < x < 0.5$ undergo transitions from a PM-insulating to a FM-metallic state at temperatures between 175 and 230 K, according to x .

In this context, we have focused on charge-ordered and close to metal-insulator transition manganites in order to evaluate them as dielectric materials alternative to classical ferroelectrics.

2. EXPERIMENTAL

2.1. Material synthesis

Polycrystalline samples were prepared by grinding highly pure and dried La_2O_3 , CaO , and Mn_2O_3 in an agate ball-mortar. These oxides were mixed in three different proportions according to the composition of $\text{La}_{0.60}\text{Ca}_{0.40}\text{MnO}_3$ (LC40), $\text{La}_{0.55}\text{Ca}_{0.45}\text{MnO}_3$ (LC45) and $\text{La}_{0.50}\text{Ca}_{0.50}\text{MnO}_3$ (LC50). The obtained powders were compacted using conventional uniaxial pressing at 5 ton/cm². Successive thermal treatments at 1200 and 1300°C in air with intermediate grindings of the pellets were performed. The samples calcined at 1300°C were ground and part of the resulting powder was uniaxially pressed at 10 ton/cm² into pellets of 5 mm diameter and 1 mm height. The remaining powder was uniaxially pressed at 5 ton/cm² into pellets of 10 mm diameter and 1 mm height. Both types of pellets were sintered for 24 h at 1400°C in air.

2.2. Structural and microstructural characterization

Phase evolution of the samples was followed by X-ray diffraction (XRD) using a Philips PW1710 diffractometer equipped with a Cu anode, a proportional counter and a graphite monochromator. Micrographs of the samples were taken by scanning electron microscopy (SEM) using a LEO-435VP microscope. Oxygen content of each sample was analyzed by iodometric titrations.

2.3. Electrical and magnetic characterization

Magnetization between 5 and 300 K was measured in a commercial SQUID magnetometer. Measurements after both ZFC (zero-field cooling) and FC (field cooling) were carried out applying a magnetic field of 100 Oe, under static heating. In the case of ZFC the sample was cooled up to 5 K without applying a magnetic field, while for FC curves a magnetic field of 100 Oe was applied during the cooling.

Four-probe DC resistivity (ρ) measurements were taken during dynamic heating between 80 and 350 K. The samples were cut in uniform bars and contacts of silver were used in order to attach Cu connections to them.

Complex dielectric permittivity was measured at frequencies ranging from 20 to 1·10⁶ Hz using a home-made device coupled to an Agilent 4284A LCR-meter. A parallel-plate capacitor was mounted in an aluminum box refrigerated with liquid N₂, coupled to a temperature controller able to measure between 90 and 350 K. The measurements were taken during static heating of the samples. Electrical contacts between the electrodes and samples were assured by sputtering with gold both material surfaces.

3. RESULTS AND DISCUSSION

Figure 1 shows the XRD patterns of the synthesized materials. In each case, all the diffraction peaks belong to the desired phases, confirming the completion of the solid-state reaction and the absence of spurious phases. Structural parameters of the formed phases are in good agreement with those reported by crystallographic databases (13). Iodometric titrations resulted in oxygen contents very close to the stoichiometric value (3.00) for all the studied compositions.

Micrographs of the sintered materials are observed in Figure 2. Differences in microstructure are observed between

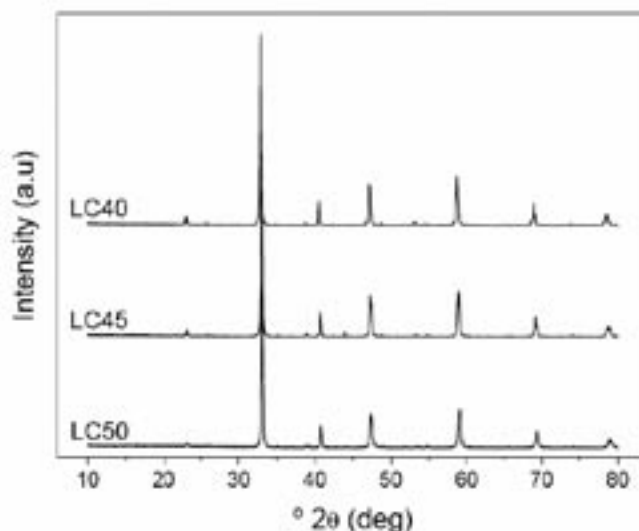


Fig. 1- XRD patterns for samples LC40, LC45 and LC50 calcined at 1400°C.

samples compacted at 5 and 10 ton/cm². In the first case, intergranular porosity with average size of 1-2 μm can be noticed. For the powders formed at higher pressure, a very low porosity is observed, showing an almost complete sintering. The higher compaction degree obtained by pressing at 10 ton/cm² produces a more efficient mass transport during the heating, leading to more homogeneous microstructures. Also, slightly larger grains are obtained for compositions with lower Ca content, which could suggest a correlation between the sintering rate and the La/Ca ratio for these manganites. Since the better microstructures were obtained for the samples

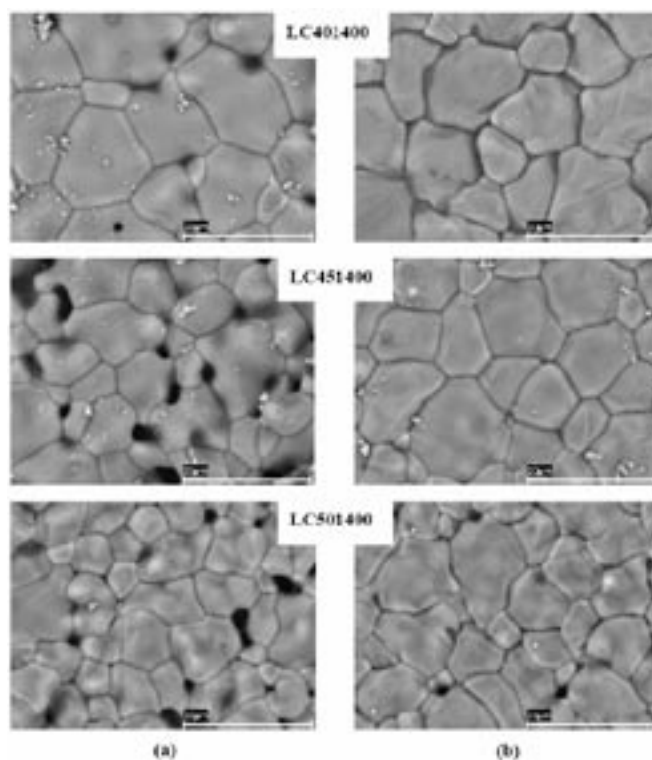


Fig. 2- SEM micrographs of samples LC40, LC45 and LC50 uniaxially pressed at 5 (a) and 10 (b) ton/cm². All the pellets were sintered at 1400°C. Bar: 20μm.

pelletized at higher pressures, only the magnetic and dielectric properties of these materials were measured.

Figure 3 shows the magnetic susceptibility (χ) as a function of temperature. Samples LC40 and LC45 show a typical FM-PM transition at Curie temperatures (T_c) of 265 and 250 K, respectively. For sample LC50 an AFM-FM transition at about 185 K and a FM-PM transition at 220 K are observed. All these temperatures coincide with those obtained from the magnetic phase diagram (10), confirming the good quality of the synthesized materials. The large hysteresis exhibited between ZFC and FC curves can be explained taking into

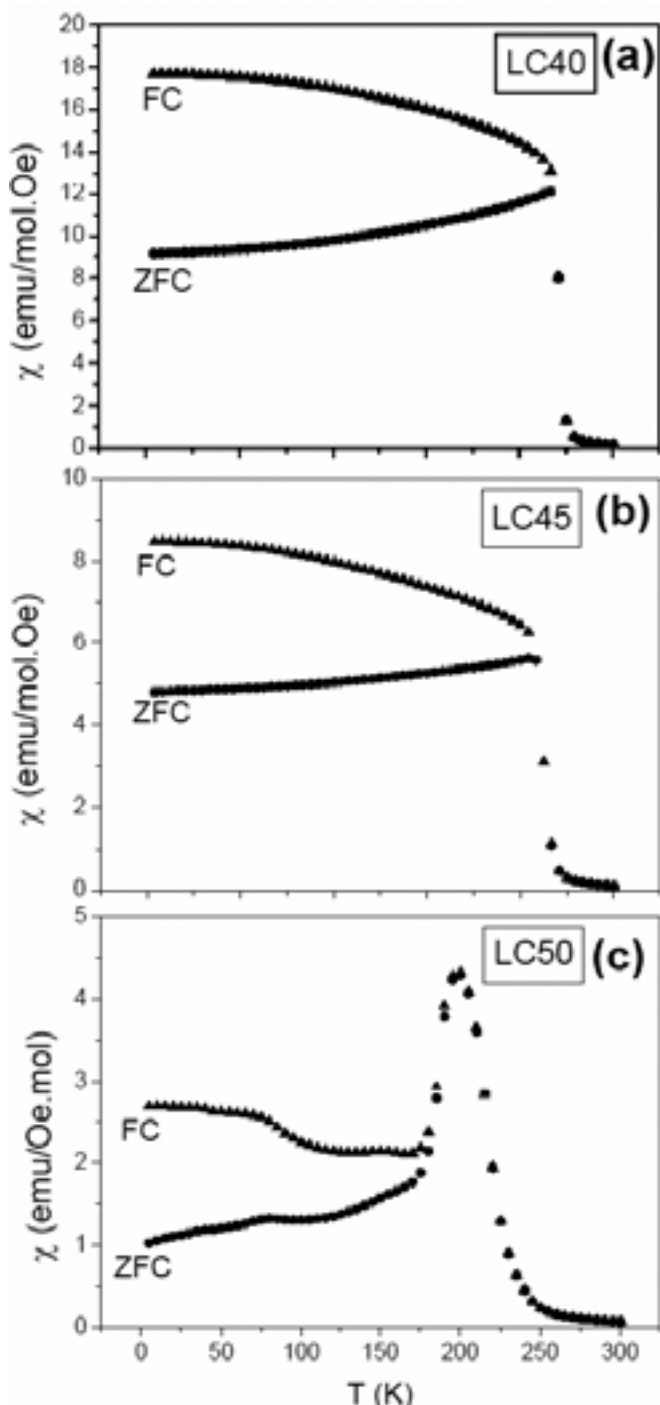


Fig. 3- Magnetic susceptibility (χ) as a function of temperature for sintered samples LC40 (a), LC45 (b) and LC50 (c).

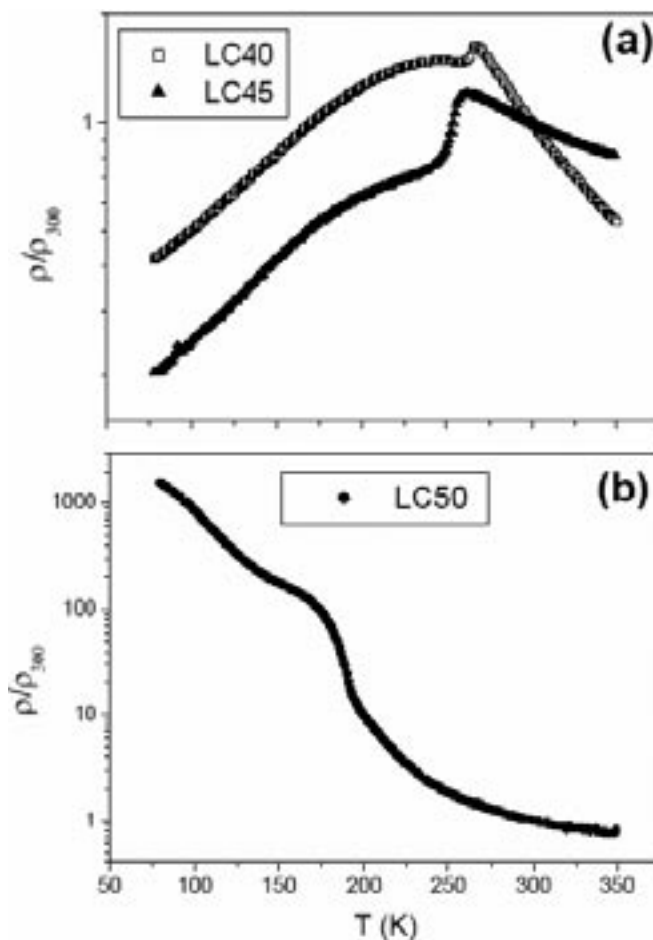


Fig. 4- DC resistivity (ρ) vs. temperature for samples LC40 y LC45 (a) and LC50 (b).

account the nature of these magnetic transitions, in which the transformation from PM to FM state involves a progressive appearance of FM domains. Upon cooling, the application of a magnetic field (FC curves) can enlarge the size of these domains, provoking higher magnetic susceptibilities than those displayed for ZFC curves at temperatures below T_c .

DC resistivity as a function of temperature is shown in Figure 4. The resistivity values represented in this figure are relative to those measured at 300 K for LC40, LC45 and LC50 (which are $2.8 \cdot 10^{-2}$, $6.3 \cdot 10^{-3}$ and $4.8 \cdot 10^{-3} \Omega \cdot \text{cm}$, respectively). For samples LC40 and LC45 metal-insulator transitions are observed at 264 and 251 K, respectively. Taking into account the magnetic behavior (Fig. 3) we can conclude that upon heating these systems are changing from a ferromagnetic-metallic to a paramagnetic-insulating (or semiconducting) state. In contrast, sample LC50 always shows values of $\delta\rho/\delta T < 0$, which indicates an insulating (or semiconducting) response in the entire temperature range. However, a wide and small band centered at $T \sim 180$ K can be noticed, as a consequence of a charge-order transition, according to previous reports (10-12).

Figure 5 shows the real part of the relative permittivity (dielectric constant, ϵ'_r) of the samples as a function of frequency at several temperatures. For the three compositions, a plateau of ϵ'_r between $1 \cdot 10^5$ and $1 \cdot 10^6$ can be observed at frequencies from 300 to $3 \cdot 10^5$ Hz. These abnormally high dielectric constant values are the result of the combination of intrinsic and extrinsic effects. The first ones are related to the

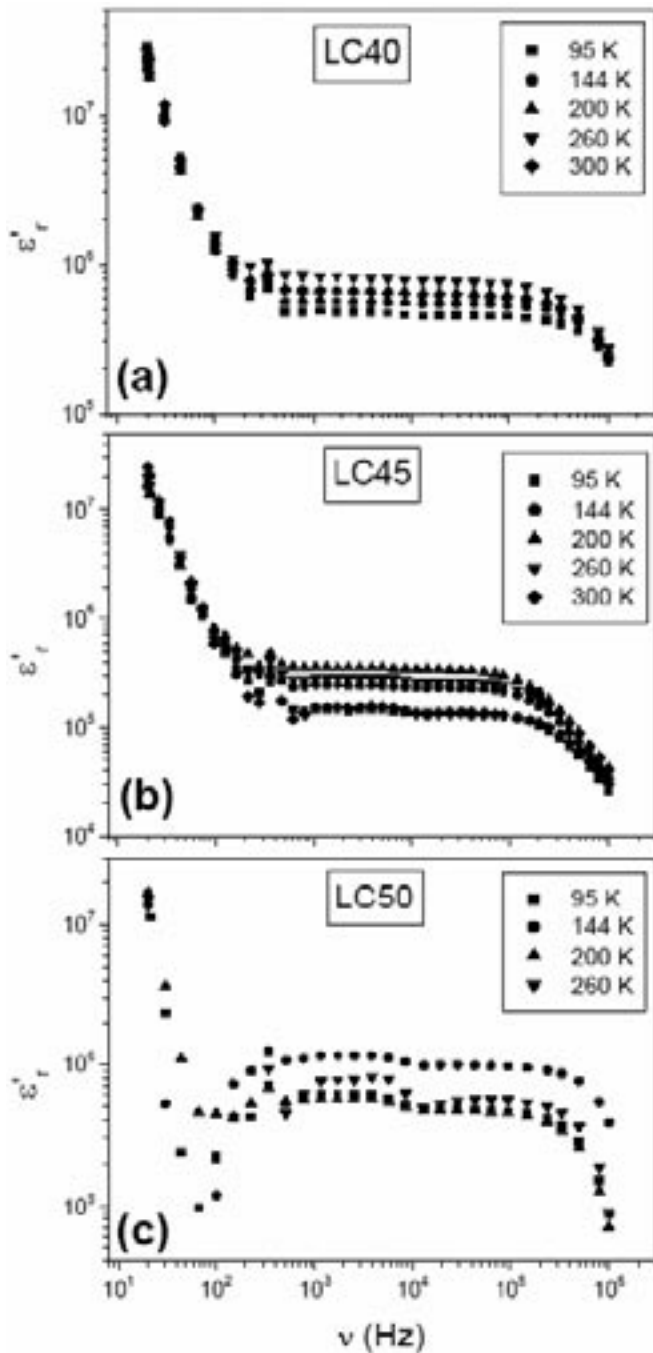


Fig. 5- Real part of the complex relative dielectric permittivity (ϵ'_r) vs frequency at selected temperatures for LC40 (a), LC45(b) and LC50 (c).

charge condensation that takes place in some systems with cations of variable valence, such as Ni^{2+} - Ni^{3+} and Mn^{3+} - Mn^{4+} (8,9). The extrinsic factors are associated to the interfacial polarization produced in grain boundaries and contacts sample-electrode (7). At the highest frequencies a drop of dielectric constant is observed for all the temperatures, suggesting the relaxation of these interfacial phenomena. In this way, in order to evaluate both contributions, the realization of dielectric measurements at higher frequencies would be necessary. In spite of this, a linear extrapolation of

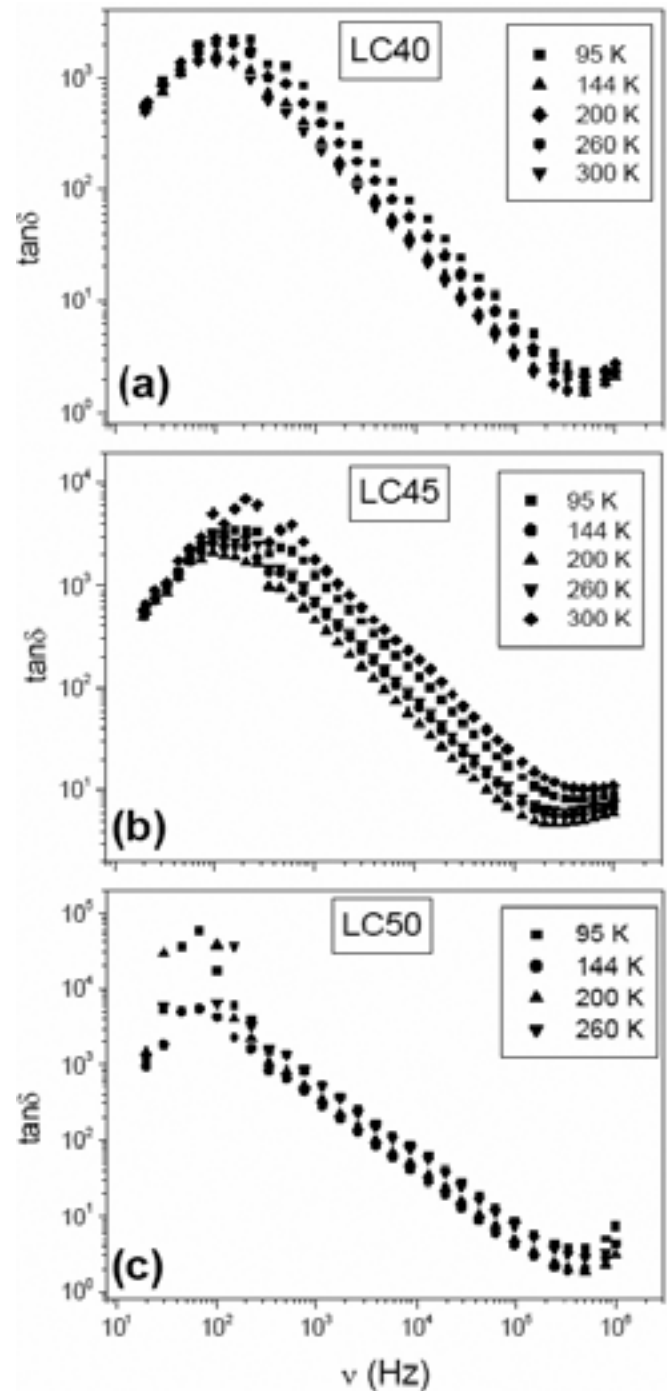


Fig. 6- Loss tangent ($\tan\delta$) vs. frequency at several temperatures for LC40 (a), LC45 (b) and LC50 (c).

the curves up to $1 \cdot 10^9$ Hz (a enough high frequency to consider a complete relaxation) may be a good approximation to intrinsic ϵ'_r values (14). This gives dielectric constants of about 50 for these manganites. Therefore, the extrinsic effects play an extremely significant role in the dielectric response of this kind of materials, specially at low frequencies.

In Figure 6 dielectric loss tangent vs frequency is plotted. Very high values are observed at low frequencies for all the prepared manganites. In fact, values as high as $1 \cdot 10^4$ are reached for LC50. At higher frequencies $\tan\delta$ exponentially decreases up to reach values ranged between 2 and 10. These high dielectric

losses are a direct consequence of the semiconducting nature of these materials, which have relatively high DC conductivities. The high $\tan\delta$ values are a serious obstacle for the application of these manganites as dielectric materials. However, this limitation could be overcome using these compounds in composite materials together with insulating oxides, such as Al_2O_3 or SiO_2 . A comparison between $\tan\delta$ curves of LC40, LC45 and LC50 reveals that the higher Ca^{2+} content the higher dielectric loss. This could be explained considering that the Ca^{2+} content is proportional to the hole concentration, since each Ca^{2+} ion produces the loss of an electron from a Mn^{3+} ion, leading to an increase of the free carrier conduction.

The dependence of the dielectric constant with temperature

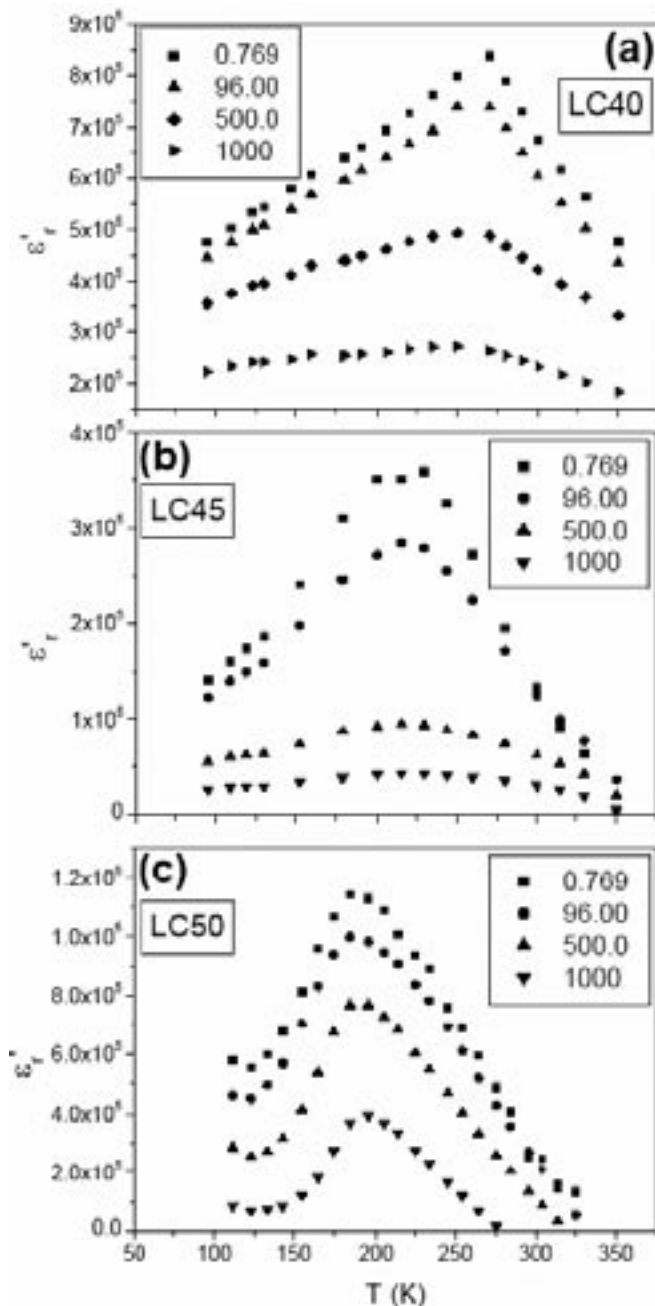


Fig. 7- ϵ' as a function of temperature at selected frequencies for LC40 (a), LC45 (b) and LC50 (c). The frequency values are given in kHz.

is shown in Figure 7. A clear maximum (of increasing intensity for lower frequencies) is observed for all the samples. For LC50 this maximum is centered on 185 K, which is the charge ordering temperature, according to Fig. 4b. A similar behavior was recently observed in $\text{La}_{1.5}\text{Sr}_{0.5}\text{NiO}_4$ which was attributed to a rearrangement from the checkerboard-type charge ordering to the stripe-type one (15). However, for LC40 and LC45 these peaks are observed too, in spite of these samples does not show charge ordering. In these cases the ϵ'_r peaks appear at temperatures very close to their corresponding metal-insulator transitions, as shown in Fig. 4a. All this evidence seems to indicate the existence of a link between the electronic state of the material and its dielectric function. This experimental observation could motivate further studies about similar systems that exhibit high dielectric constants by non-ferroelectric mechanisms.

4. SUMMARY

The synthesized materials ($\text{La}_{0.60}\text{Ca}_{0.40}\text{MnO}_3$, $\text{La}_{0.55}\text{Ca}_{0.45}\text{MnO}_3$ and $\text{La}_{0.50}\text{Ca}_{0.50}\text{MnO}_3$) show huge dielectric constants (10^5 - 10^6) in a wide range of frequencies and temperatures. These values are mainly the result of a strong extrinsic contribution (interfacial polarization), besides an intrinsic effect due to charge condensation.

The dielectric constant of these manganites exhibits a maximum in temperature. For $\text{La}_{0.60}\text{Ca}_{0.40}\text{MnO}_3$ and $\text{La}_{0.55}\text{Ca}_{0.45}\text{MnO}_3$ this is associated to their respective metal-insulator transitions, while for $\text{La}_{0.50}\text{Ca}_{0.50}\text{MnO}_3$ the peak is related to a charge-order rearrangement.

Although the high dielectric losses observed for these manganites make difficult its application as dielectric materials, they could be used for the synthesis of composite materials together with insulating matrixes.

ACKNOWLEDGEMENTS

This work was financed by MAT2004-05130 from MEC (Spain). PMB thanks CONICET and Fundación Antorchas (Argentina) for grants.

REFERENCES

1. R.J. Cava, Dielectric materials for applications in microwave communications, *J. Mater. Chem.* 11 54-62 (2001).
2. B.G. Kim, S.M. Cho, T-Y. Kim and H.M. Jang, Giant dielectric permittivity observed in Pb-based perovskite ferroelectrics, *Phys. Rev. Lett.* 86 3404-3406 (2001).
3. C.C. Homes, T. Vogt, M. Shapiro and A.P. Ramirez, Optical response of high-dielectric-constant perovskite-related oxide, *Science* 293 673-676 (2001).
4. C. Pecharrmán, F. Esteban-Betegón, J.F. Bartolomé, S. López-Esteban and J.S. Moya, New percolative BaTiO_3 -Ni composites with a high and frequency-independent dielectric constant ($\epsilon_r = 80\,000$), *Adv. Mater.* 13 1541-1544 (2001).
5. J. Wu, C.-W. Nan, Y. Lin and Y. Deng, Giant dielectric permittivity observed in Li and Ti doped NiO, *Phys. Rev. Lett.* 89 217601 (2002).
6. D.C. Sinclair, T.B. Adams, F.D. Morrison and A.R. West, $\text{CaCu}_2\text{Ti}_2\text{O}_{12}$: one-step internal barrier layer capacitor, *Appl. Phys. Lett.* 80 2153-2155 (2002).
7. P. Lunkenheimer, V. Bobnar, A.V. Pronin, A.I. Ritus, A.A. Volkov and A. Loidl, Origin of apparent colossal dielectric constants, *Phys. Rev. B* 66 052105 (2002).
8. C. Jardón, F. Rivadulla, L.E. Hueso, A. Fondado, J. Rivas, M.A. López Quintela, R. Zysler, M. T. Causa and P. Sande, Experimental study of charge ordering transition in $\text{Pr}_{0.67}\text{Ca}_{0.33}\text{MnO}_3$, *J. Magn. Magn. Mater.* 195-197 475-476 (1999).

9. J. Rivas, B. Rivas-Murias, A. Fondado, J. Mira and M.A. Señaris-Rodríguez, Dielectric response of the charge-ordered two-dimensional nickelate $\text{La}_{1-x}\text{Sr}_x\text{NiO}_4$, *Appl. Phys. Lett.* 85 6224-6226 (2004).
10. S.-W. Cheong and C.H. Chen, Colossal magnetoresistance, charge ordering and related properties of manganese oxides, 241-266, C.N.R. Rao and B. Raveau Ed., World Scientific, Singapore, 1998.
11. P. Levy, F. Parisi, G. Polla, D. Vega, G. Leyva and H. Lanza, Controlled phase separation in $\text{La}_{0.50}\text{Ca}_{0.50}\text{MnO}_3$, *Phys. Rev. B* 62 6437-6441 (2000).
12. M. Roy, F.J. Mitchell, A.P. Ramírez and P.E. Schiffer, A study of the magnetic and electrical crossover region of $\text{La}_{0.5\pm\delta}\text{Ca}_{0.5\pm\delta}\text{MnO}_3$, *J. Phys.: Condens. Matter.* 11 4834-4859 (1999).
13. ICSD, Inorganic Crystal Structure Database 2004.
14. A. von Hippel, *Dielectrics and Waves*, Artech House, London, 1954.
15. R. Kajimoto, K. Ishizaka, H. Yoshizawa, Y. Tokura, Spontaneous rearrangement of the checkerboard charge order to stripe order in $\text{La}_{1-x}\text{Sr}_x\text{NiO}_4$, *Phys. Rev. B* 67 014511 (2003).

Recibido: 15.07.05

Aceptado: 09.02.06

